CARBON 49 (2011) 1362–1366

available at www.sciencedirect.com

ScienceDirect

journal homepage: www.elsevier.com/locate/carbon

Electronic structure of graphite oxide and thermally reduced graphite oxide

Da Zhan [a], Zhenhua Ni [b], Wei Chen [c,d], Li Sun [a], Zhiqiang Luo [a], Linfei Lai [a], Ting Yu [a], Andrew Thye Shen Wee [c], Zexiang Shen [a,*]

[a] Division of Physics and Applied Physics, School of Physical and Mathematical Sciences, Nanyang Technological University, Singapore 637371, Singapore

[b] Department of Physics, Southeast University, Nanjing 211189, China

[c] Department of Physics, Faculty of Science, National University of Singapore, 2 Science Drive 3, Singapore 117542, Singapore

[d] Department of Chemistry, Faculty of Science, National University of Singapore, 3 Science Drive 3, Singapore 117543, Singapore

ARTICLE INFO

Article history:
Received 24 August 2010
Accepted 1 December 2010
Available online 4 December 2010

ABSTRACT

We present the electronic structure evolution from graphite oxide to thermally reduced graphite oxide. Most functional groups were removed by thermal reduction as indicated by high resolution X-ray photoelectron spectroscopy, and the electrical conductivity increased 6 orders compare with the precursor graphite oxide. X-ray absorption spectroscopy reveals that the thermally reduced graphite oxide shows several absorption peaks similar to those of pristine graphite, which were not observed in graphite oxide or chemically reduced graphite oxide. This indicates the better restoration of graphitic electronic conjugation by thermal reduction. Furthermore, the significant increased intensity of Raman 2D band of thermally reduced graphite oxide compared with graphite oxide also suggests the restoration of graphitic electronic structure (π orbital). These results provide useful information for fundamental understanding of the electronic structure of graphite oxide and thermally reduced graphite oxide.

1. Introduction

Graphite oxide (GO) is a functional groups rich carbonaceous layered material [1,2]. It is a non-stoichiometric compound consists of various functional groups. The epoxy and hydroxyl groups randomly interspersed on the top and bottom surfaces of each graphene sheet, while carboxyl and carbonyl groups normally locate at edges [1–4]. Despite the presence of functional groups, the layered structure of GO is well preserved with AB stacking order [3,5]. GO is insulator, but reduced graphite oxide (RGO) is good conductor with conductivity 4–6 orders higher than that of GO due to the restoration of sp^2-carbon networks [1,6–9]. RGO can be prepared into large size films with high conductivity and transparency for practical applications [7,10]. For example, RGO film was used as transparent and conductive electrodes for dye-sensitized solar cell [8] and ultra-capacitor applications [11].

Although the recent progress on processing RGO film for various practical applications have been reported [7,8,10–12], the fundamental understanding of the electronic structure of this carbon-based composite is still lacking. Soft X-ray absorption spectroscopy (XAS) is a very reliable tool to investigate the electronic structure (unoccupied states above Fermi level) of carbon-based materials [13–16]. However, reports on electronic structure of GO and RGO probed by XAS are very limited [17–19]. To our best knowledge, there are no relevant reports on thermally reduced graphite oxide (tRGO) even though it is considered as the most simple and effective

* *Corresponding author:* Fax: +65 6795 7981.
E-mail address: zexiang@ntu.edu.sg (Z. Shen).
0008-6223/$ - see front matter
doi:10.1016/j.carbon.2010.12.002

method to achieve best restoration of sp^2-carbon structures compare with normal chemically reduced graphite oxide (tRGO) [6,7]. In this work, X-ray photoelectron spectroscopy (XPS), conductivity measurement and Raman spectroscopy were used to assist XAS to investigate electronic structure evolution from GO to tRGO.

2. Experimental

Graphite oxide was synthesized from natural graphite powder by conventional modified Hummers method [5]. Two pieces of paper-like structured GO films with size of ~5 × 5 mm and thickness of ~1 μm were prepared [20]. One of the GO films was reduced by H_2/Ar (1:2) airflow at 950 °C for 30 min (tRGO). The heating and cooling rates were keeping at ~5 °C/min. The carbon-related chemical species of GO and tRGO were characterized by high resolution XPS using Kratos Axis Ultra DLD (delay line detector) spectrometer equipped with a monochromatic Al Kα X-ray source (1486.6 eV) with resolution of 0.1 eV. The conductivity of GO and tRGO films was measured by Keithley 2612A electrical measurement system. Raman spectra were recorded by (1) WITEC CRM200 system (excitation laser energy is 2.33 eV); (2) Renishaw system (excitation laser energies are 1.58 and 3.81 eV, respectively). The near edge X-ray absorption fine structure (NEXAFS) measurements were carried out at the Surface, Interface, and Nanostructure Science (SINS) beamline of the Singapore Synchrotron Light Source, using total-electron yield (TEY) mode and linear p-polarized light with photon energy resolution of 0.1 eV.

3. Results and discussion

High resolution XPS spectra of C 1s region of GO and tRGO are shown in Fig. 1, while the detailed information on the portion of deconvoluted components is shown in Table 1. It can be seen clearly that GO shows three most prominent deconvoluted components, with one of them assigned to sp^2-C 1s (at ~285 eV), and the other two assigned to species of C–O (hydroxyl and epoxy) and C=O (carboxyl) with binding energy of ~287 and ~289 eV, respectively [1,3,7]. This clearly shows high degree oxidation of GO. For tRGO, most chemically attached functional groups were successfully removed by thermal reduction, and the portion of sp^2 hybridized carbon species obviously increased as shown in Fig. 1b. Furthermore, the full width of half maximum (FWHM) of sp^2 carbon peak is very small (~1 eV), and it is similar to that of the previously reported tRGO [7].

I–*V* curves of GO and tRGO are shown in Fig. 2. The differential conductivity of GO is $\sim 10^{-4}$ S/cm at bias voltage of 3 V, while the conductivity of tRGO is ~100 S/cm, approximately 6 orders higher than that of GO. The dramatic enhancement of conductivity of tRGO also infers the removal of oxygenated functional groups and the restoration of sp^2 hybridized carbon component, which is in consistent with the XPS results.

Raman spectra of GO and tRGO are shown in Fig. 3. There are two main prominent peaks for both GO and tRGO samples, assigned to G band (~1580 cm^{-1}) and D band (1310–1430 cm^{-1}, depends on the excitation laser energy), which are E_{2g} vibrational mode in-plane and A_{1g} breathing mode, respectively [21]. G band is Raman active for sp^2 hybridized carbon-based material, while D band is activated only if defects participate the double resonance Raman scattering near K point of Brillouin zone [22]. Although chemical components of GO is significantly different from that of tRGO, Raman spectra show neglectable changes on the intensity ratio of I_D/I_G between GO and tRGO (Fig. 3). Therefore, our results indicate that the average size of sp^2 domains does not change significantly from GO to tRGO as the intensity ratio of I_D/I_G is normally used for estimating the sp^2 domain size of graphite-based materials. It is reasonable that though thermal reduction can remove the functional groups from GO, the exfoliation of GO is inevitable during the thermal reduction [1,6], and these two factors make the sp^2 domain size of GO does not change significantly after reduction. Besides G and D bands, there are two Raman bands with weaker intensity called 2D and D + G locate at

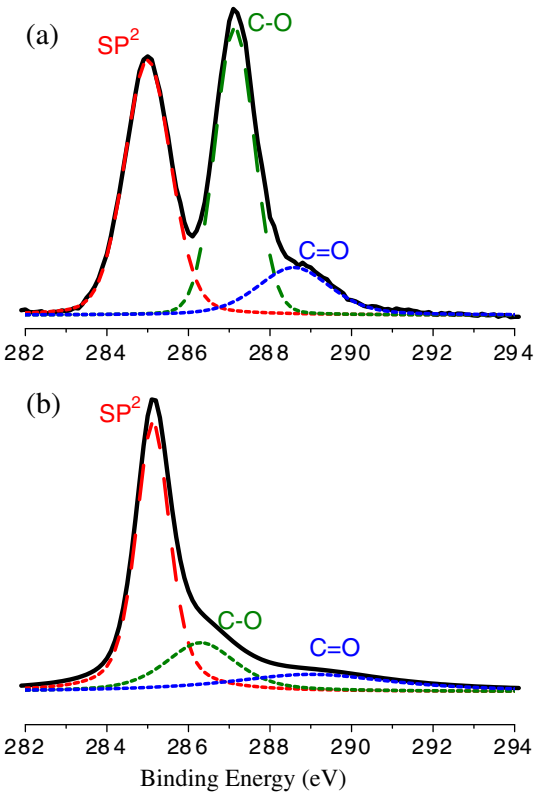

Fig. 1 – High resolution XPS spectra of GO (a) and tRGO (b). The black solid lines are original spectra; the deconvoluted dashed lines in red, green and blue are assigned to sp^2-C, C–O (hydroxyl and epoxy groups), C=O (carboxyl groups), respectively. (For interpretation of the references to colour in this figure legend, the reader is referred to the web version of this article.)

Table 1 – The portion of chemical species for GO and tRGO based on XPS results.

	GO	tRGO
sp^2 (C–C)%	45 ± 5	74 ± 5
C–O%	41 ± 5	14 ± 3
C=O%	14 ± 2	12 ± 2

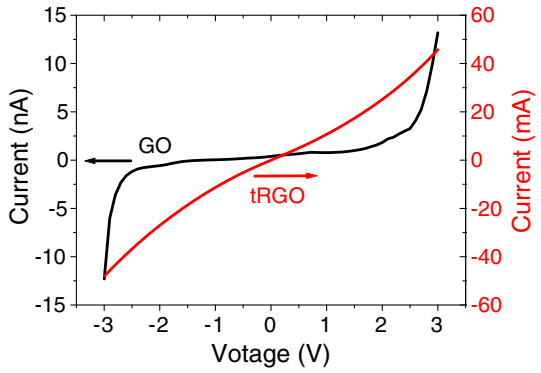

Fig. 2 – I–V curves of GO (black line) and tRGO (red line). (For interpretation of the references to colour in this figure legend, the reader is referred to the web version of this article.)

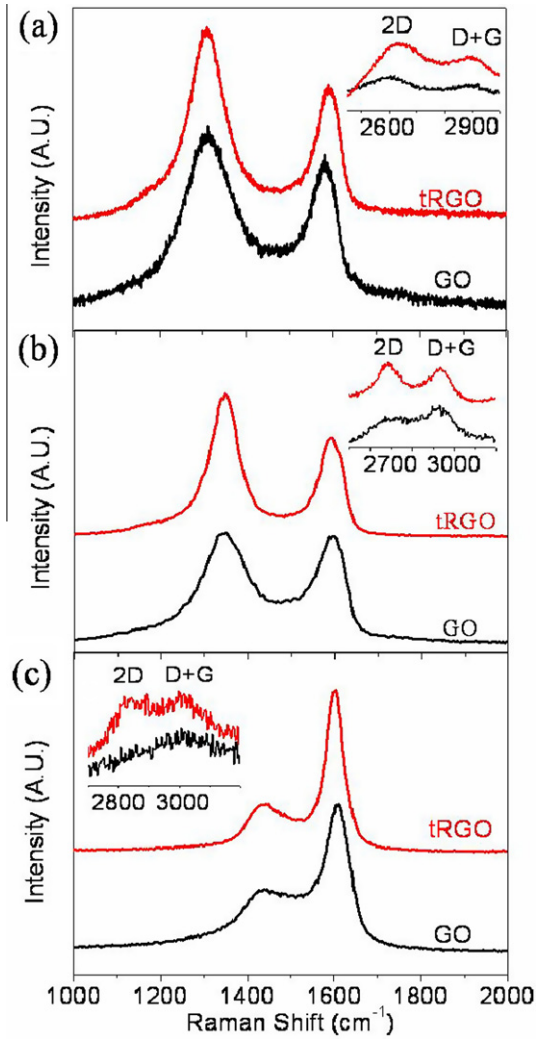

Fig. 3 – Raman spectra for GO and tRGO excited by various excitation laser energies (wavelengths): (a) 1.58 eV (785 nm), (b) 2.33 eV (532 nm), (c) 3.81 eV (325 nm). Insets are 2D and D + G range for GO and tRGO (background removed).

2700–3000 cm^{-1} as shown in insets of Fig. 3. 2D band is Raman active for crystalline graphitic materials and it is sensitive to the π band in the graphitic electronic structure, while the combination mode of D + G is induced by disorder [22]. 2D and D + G bands are normally ignored on the studies of GO and RGO because of the weak intensity [1,6,9,19,23]. Here, we found that it is very easy to distinguish the electronic conjugation of GO and tRGO by comparing these two bands, in which the obvious enhancement of 2D intensity of tRGO compared with GO can be clearly observed using various excitation laser energies (insets of Fig. 3). The intensity ratios of I_D/I_G and I_{2D}/I_{D+G} are also shown in Table 2. The data also shows that from GO to tRGO, the I_{2D}/I_{D+G} changed more significantly than I_D/I_G, and the dramatically increased I_{2D}/I_{D+G} from GO to tRGO using various excitation laser energies suggests that the recovery of graphitic electronic conjugation for tRGO.

In addition to Raman spectroscopy, NEXAFS measurement is an effective method for analyzing unoccupied electronic structure of carbon related materials [13–16]. Carbon K-edge NEXAFS (1s–π* and 1s–σ* locate at ~285 and 293 eV, respectively) spectra in TEY mode for GO and tRGO are shown in Fig. 4. The two-dimensional nature of graphitic material is supposed to have strong directionality of the orbitals: σ orbitals lie within the basal plane and π orbitals are directed perpendicular to the basal plane. Therefore, XAS is angle dependent for the sp^2-carbon-based materials with layered structure. The NEXAFS for GO and tRGO were using linear polarized X-ray beam with incident beam angle of $\theta = 90°$ (perpendicular) and $\theta = 20°$ (parallel dominate) respect to substrate (inset of Fig. 4). For ideal highly ordered pyrolytic graphite (HOPG) or graphene, as the E vector is parallel to the basal plane when the incident beam angle is 90°, thus the transition of 1s–π* should be quenched as the π final states cannot be selected [14]. In our experiment, the 1s–π* transition is not fully quenched for normal incidence ($\theta = 90°$), but the intensity is obviously decreased compared with parallel incidence ($\theta = 20°$) (Fig. 4b). This is similar to the results reported recently by Lee et al. [19]. However, the incident-angle dependence of 1s–π* transition intensity for GO and tRGO is rather weak compared to that of HOPG. This suggests that the GO and tRGO are not perfectly flat 2-D materials but present wave-like 2-D structure with periodic fluctuation, probably originating from the coexistence of different micro-domains, the rather disordered stacking of GO and tRGO planes compared to that of HOPG, as well as the disordering induced by the oxidation processes [20]. Furthermore, the hydroxyl and epoxy groups distributed randomly on top and bottom of basal plane of each graphene layer would pull the bonded carbon atoms up and down with respect to the basal plane. For 1s–σ* transition, the intensity becomes much stronger for tRGO when the incident beam angle is changed from $\theta = 20°$ to $\theta = 90°$, but there is only small enhancement for GO. This is another evidence to show that only small amount of σ orbitals keep intact for GO because of the strong oxidation, while the intact σ orbitals increased dramatically with the restoration of sp^2 hybridized carbon network by thermal reduction. A shoulder peak at 292 eV of tRGO for $\theta = 90°$ should be excitonic state, the existence of this excitonic state indicates that tRGO consist of a large number of sp^2 hybridized carbon atoms as this peak is usually observed for pristine graphite [17] and cRGO [19]. Here, we should emphasize that despite the thermal reduction process removed most functional groups, the tRGO can only be

Table 2 – Intensity ratios of I_D/I_G and I_{2D}/I_{D+G} for GO and tRGO excited by various excitation laser energies.

Laser energy (eV)	GO (I_D/I_G)	tRGO (I_D/I_G)	GO (I_{2D}/I_{D+G})	tRGO (I_{2D}/I_{D+G})
1.56	2.27 ± 0.12	2.44 ± 0.11	2.09 ± 0.22	3.91 ± 0.27
2.33	2.11 ± 0.10	2.01 ± 0.13	0.70 ± 0.15	1.52 ± 0.20
3.81	1.54 ± 0.05	1.05 ± 0.06	0.17 ± 0.05	0.49 ± 0.10

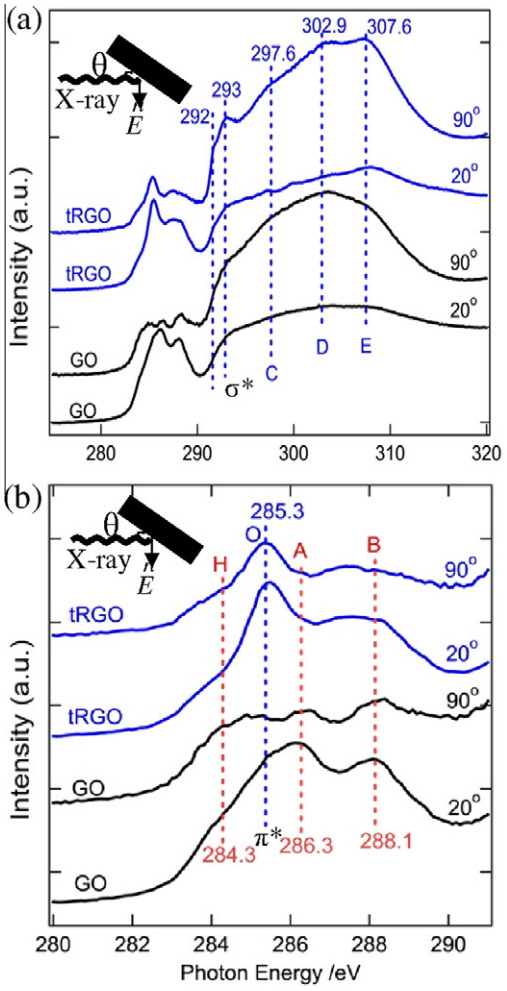

Fig. 4 – (a) C K-edge XAS of GO and tRGO for incident beam angle of $\theta = 20°$ and $\theta = 90°$, respectively. (b) The enlarged region of 280–291 eV.

considered as a mixture of the graphite-like species and other unspecified components as the weak 1s–σ* and 1s–π* peaks compare to the background absorption.

In Fig. 4b (Enlarged region of 280–291 eV), besides the absorption peak O induced by sp^2-C 1s–π* transition at 285.3 eV, two additional absorption peaks A and B at 286.3 and 288.1 eV can be clearly observed for GO with both incident beam angle of $\theta = 20°$ and 90°, respectively. Peak A can be assigned to 1s–π* (C–O) transition as the hydroxyl and epoxy functional groups chemically attached to basal plane of each graphene layer [24]; peak B can be assigned to 1s–π* (C=O) as the existence of carboxyl and carbonyl groups [18]. There is one more peak H locates at 284.3 eV for GO, about 1 eV below 1s–π* (sp^2). This peak is possibly attributed to edge-derived electronic state as similar structure has been observed in nanographite [25] and single layer graphene [26], respectively.

At higher photon energy range, the 1s–σ* transition around 293 eV is assigned to the final state of 1s–σ_1* and 1s–σ_2* at Brillouin zone region Γ–Q [14]. In addition to this prominent transition, XAS for single crystalline graphite usually can resolve absorption transitions from ground state 1s to other σ* subband states which contain high unoccupied density of states at about 10–30 eV above the Fermi level [14]. In our experiment, three additional peaks C–E, respectively, locate at 297.6, 302.9 and 307.6 eV are observed for tRGO (Fig. 4a). These peaks were also observed for single crystalline graphite locate at 297.8, 303.5 and 307.5 eV, respectively [14]. The obvious enhanced signals for peaks C–E at incident beam angle of $\theta = 90°$ than that of $\theta = 20°$ further confirms that C–E are due to transitions from 1s state to other σ* subband states. On the other hand, there are no such noticeable peaks for GO and they were not observed for cRGO as reported elsewhere [19]. Therefore, tRGO presents more similar electronic structure to pristine graphite than that of cRGO. This indicates the better restoration of graphitic electronic conjugation by thermal reduction than chemical reduction. The better restoration of electronic conjugation of tRGO compared with cRGO is the basic and significant evidence to explain why tRGO normally present higher electrical conductivity than that of cRGO [6,7].

4. Conclusions

In conclusion, the electronic structure of GO and tRGO is systematically studied. It is found that the comparison of Raman 2D and D + G bands can indirectly monitor the electronic structure of GO and tRGO (π orbitals). Angle dependent C K-edge NEXAFS measurement also confirmed the effective restoration of the graphitic electronic conjugation on tRGO. In addition to two prominent transition peaks 1s–π* and 1s–σ* at ~285 and 293 eV, respectively, some other peaks (at 297.6, 302.9 and 307.6 eV) were also observed, which is similar to that of pristine graphite. This indicates that the tRGO contains similar electronic structure as that of graphite, particularly the in-plane σ* subband states. These results explained the key reasons for the significant increase of electrical conductivity of tRGO.

REFERENCES

[1] Stankovich S, Dikin DA, Piner RD, Kohlhaas KA, Kleinhammes A, Jia Y, et al. Synthesis of graphene-based

nanosheets via chemical reduction of exfoliated graphite oxide. Carbon 2007;45(7):1558–65.
[2] Stankovich S, Dikin DA, Dommett GHB, Kohlhaas KM, Zimney EJ, Stach EA, et al. Graphene-based composite materials. Nature 2006;442(7100):282–6.
[3] Jeong HK, Lee YP, Lahaye R, Park MH, An KH, Kim IJ, et al. Evidence of graphitic AB stacking order of graphite oxides. J Am Chem Soc 2008;130(4):1362–6.
[4] Stankovich S, Piner RD, Nguyen ST, Ruoff RS. Synthesis and exfoliation of isocyanate-treated graphene oxide nanoplatelets. Carbon 2006;44(15):3342–7.
[5] Hirata M, Gotou T, Horiuchi S, Fujiwara M, Ohba M. Thin-film particles of graphite oxide 1: high-yield synthesis and flexibility of the particles. Carbon 2004;42(14):2929–37.
[6] Kang H, Kulkarni A, Stankovich S, Ruoff RS, Baik S. Restoring electrical conductivity of dielectrophoretically assembled graphite oxide sheets by thermal and chemical reduction techniques. Carbon 2009;47(6):1520–5.
[7] Becerril HA, Mao J, Liu Z, Stoltenberg RM, Bao Z, Chen Y. Evaluation of solution-processed reduced graphene oxide films as transparent conductors. ACS Nano 2008;2(3):463–70.
[8] Wang X, Zhi LJ, Mullen K. Transparent, conductive graphene electrodes for dye-sensitized solar cells. Nano Lett 2008;8(1):323–7.
[9] Gomez-Navarro C, Weitz RT, Bittner AM, Scolari M, Mews A, Burghard M, et al. Electronic transport properties of individual chemically reduced graphene oxide sheets. Nano Lett 2007;7(11):3499–503.
[10] Watcharotone S, Dikin DA, Stankovich S, Piner R, Jung I, Dommett GHB, et al. Graphene–silica composite thin films as transparent conductors. Nano Lett 2007;7(7):1888–92.
[11] Stoller MD, Park SJ, Zhu YW, An JH, Ruoff RS. Graphene-based ultracapacitors. Nano Lett 2008;8(10):3498–502.
[12] Wang GX, Shen XP, Yao J, Park J. Graphene nanosheets for enhanced lithium storage in lithium ion batteries. Carbon 2009;47(8):2049–53.
[13] Zhou XT, Sham TK, Wu Y, Chong YM, Bello I, Lee ST, et al. X-ray excited optical luminescence from diamond thin films: the contribution of sp(2)- and H-bonded carbon to the luminescence. J Am Chem Soc 2007;129(6):1476–7.
[14] Rosenberg RA, Love PJ, Rehn V. Polarization-dependent C(K) near-edge X-ray-absorption fine-structure of graphite. Phys Rev B 1986;33(6):4034–7.
[15] Carlisle JA, Shirley EL, Hudson EA, Terminello LJ, Callcott TA, Jia JJ, et al. Probing the graphite band-structure with resonant soft-X-ray fluorescence. Phys Rev Lett 1995;74(7):1234–7.
[16] Banerjee S, Hemraj-Benny T, Sambasivan S, Fischer DA, Misewich JA, Wong SS. Near-edge X-ray absorption fine structure investigations of order in carbon nanotube-based systems. J Phys Chem B 2005;109(17):8489–95.
[17] Jeong HK, Noh HJ, Kim JY, Jin MH, Park CY, Lee YH. X-ray absorption spectroscopy of graphite oxide. EPL 2008;82(6):67004.
[18] Jeong HK, Colakerol L, Jin MH, Glans PA, Smith KE, Lee YH. Unoccupied electronic states in graphite oxides. Chem Phys Lett 2008;460(4–6):499–502.
[19] Lee V, Whittaker L, Jaye C, Baroudi KM, Fischer DA, Banerjee S. Large-area chemically modified graphene films: electrophoretic deposition and characterization by soft X-ray absorption spectroscopy. Chem Mater 2009;21(16):3905–16.
[20] Dikin DA, Stankovich S, Zimney EJ, Piner RD, Dommett GHB, Evmenenko G, et al. Preparation and characterization of graphene oxide paper. Nature 2007;448(7152):457–60.
[21] Ferrari AC, Robertson J. Interpretation of Raman spectra of disordered and amorphous carbon. Phys Rev B 2000;61(20):14095–107.
[22] Pimenta MA, Dresselhaus G, Dresselhaus MS, Cancado LG, Jorio A, Saito R. Studying disorder in graphite-based systems by Raman spectroscopy. Phys Chem Chem Phys 2007;9(11):1276–91.
[23] Kudin KN, Ozbas B, Schniepp HC, Prud'homme RK, Aksay IA, Car R. Raman spectra of graphite oxide and functionalized graphene sheets. Nano Lett 2008;8(1):36–41.
[24] Francis JT, Hitchcock AP. Inner-shell spectroscopy of para-benzoquinone, hydroquinone, and phenol – distinguishing quinoid and benzenoid structures. J Phys Chem 1992;96(16):6598–610.
[25] Entani S, Ikeda S, Kiguchi M, Saiki K, Yoshikawa G, Nakai I, et al. Growth of nanographite on Pt(111) and its edge state. Appl Phys Lett 2006;88(15):153126.
[26] Pacile D, Papagno M, Rodriguez AF, Grioni M, Papagno L. Near-edge X-ray absorption fine-structure investigation of graphene. Phys Rev Lett 2008;101(6):066806.